The Astrophysical Journal, 519:L1–L4, 1999 July 1

A FUNDAMENTAL TEST OF THE NATURE OF DARK MATTER

R. Benton Metcalf and Joseph Silk[1]
Departments of Physics and Astronomy and Center for Particle Astrophysics, University of California, Berkeley, Berkeley, CA 94720
Received 1998 November 4; accepted 1999 April 28; published 1999 May 19

ABSTRACT

Dark matter may consist of weakly interacting elementary particles or of macroscopic compact objects. We show that the statistics of the gravitational lensing of high-redshift supernovae strongly discriminate between these two classes of dark matter candidates. We develop a method of calculating the magnification distribution of supernovae, which can be interpreted in terms of the properties of the lensing objects. With simulated data, we show that $\gtrsim$50 well-measured Type Ia supernovae ($\Delta m \sim 0.2$ mag) at redshifts $\sim$1 can clearly distinguish macroscopic from microscopic dark matter if $\Omega_0 \gtrsim 0.2$ and all dark matter is in one form or the other.
Subject headings: cosmology: theory — dark matter — gravitational lensing

1. INTRODUCTION

The nature of dark matter (DM) poses one of the most outstanding problems in astrophysics. There are essentially two alternative hypotheses. The DM may be microscopic, consisting of weakly interacting particles such as supersymmetric neutralinos or axions, or else be macroscopic, compact objects such as primordial black holes (PBHs), brown dwarfs, or old white dwarfs (MACHOs). Big bang nucleosynthesis (BBN) puts a bound on the density in baryonic matter of $\Omega_b h^2 \lesssim 0.02$ (or $\lesssim$0.03 if one allows for inhomogeneous BBN), but the density of PBHs is not well constrained. It is possible that some hitherto unknown mechanism allows for DM that is dominated by macroscopic objects. For these reasons, direct observational constraints on macroscopic DM of any density are very important.

We propose a simple test for distinguishing macroscopic from microscopic DM. In this Letter, we consider only the opposing hypotheses that one or the other dominates. If the DM is microscopic, the component clustered into halos will lens high-redshift supernovae (SNe). If the DM is macroscopic, most light beams do not intersect any matter—i.e., there is no Ricci focusing—and the SN brightness distribution is skewed to an extent that can be quantitatively distinguished from halo lensing.

2. PROPERTIES OF THE MAGNIFICATION PROBABILITY DISTRIBUTION FUNCTION

In this Letter we consider the lensing of distant supernovae by discrete "lenses." A lens is the smallest unit of mass that acts coherently for the purpose of lensing. This could be a galaxy halo, or it could be a high-mass DM candidate such as a PBH.

We make the distinction between macroscopic and microscopic DM more quantitative by considering two mass scales. The first is defined by the requirement that the projected density be smooth on the scale of the angular size of the source. Applying this requirement to the DM about 1 Mpc from us gives a maximum mass of

$$m_s \sim 100 \text{ g} \left(\frac{\lambda_s}{\text{AU}}\right)^3 \Omega_0 h^2 f, \qquad (1)$$

where λ_s is the physical size of the source and f is a geometric factor of order unity. If the unit of DM is smaller, it is microscopic DM. Another, larger mass scale is defined by the requirement that the angular size of the source be small compared to the Einstein ring radius so that it can be considered a true point source:

$$m \gtrsim \left(\frac{D_l}{D_s}\frac{\lambda_s m^{1/2}}{R_\text{E}}\right)^2 \sim 10^{-7}\, M_\odot \left(\frac{\lambda_s}{\text{AU}}\right)^2 f, \qquad (2)$$

where D_s and D_l are the angular size distances to the source and lens. If a lens is near or below this mass, the high-magnification tail of the distribution function will be modified and the rare high-magnification events will become time dependent (Schneider & Wagoner 1987). The measured velocity of the expanding photosphere of a Type Ia SN is around $(1.0\text{–}1.4) \times 10^4$ km s^{-1} (Patat et al. 1996), which means $\lambda_s \sim (40\text{–}57)\, \Delta t$ AU week^{-1}. The SN reaches maximum light in approximately 1 week and persists for several weeks.

The background cosmology will be taken to be the standard Friedman-Lemaître-Robertson-Walker (FLRW) with the metric $ds^2 = dt^2 + a(t)^2[d\chi^2 + D(\chi)^2 d\Omega]$, where the comoving angular size distance is $D(\chi) = \{R \sinh(\chi/R), \chi, R\sin(\chi/R)\}$ $(R = |H_0(1 - \Omega_0 - \Omega_\Lambda)^{1/2}|^{-1})$ for the open, flat, and closed global geometries, respectively. Another relevant angular size distance is the Dyer-Roeder or empty-beam distance $\tilde{D}(\chi)$ (Dyer & Roeder 1974; Kantowski 1998; note difference in notation), which is the angular size distance for a beam that passes through empty space and experiences no shear.

2.1. *Magnification by a Single Lens*

Consider a single lens at a fixed coordinate distance from Earth. The path of the light is described by either of two lensing equations:

$$\boldsymbol{r}_\perp = \boldsymbol{y} - \alpha(\boldsymbol{y}, \tilde{D}_l, \tilde{D}_s), \qquad (3)$$

$$\boldsymbol{r}_\perp = [1 - \kappa_b(\chi_s)]\boldsymbol{y} - \alpha(\boldsymbol{y}, D_l, D_s), \qquad (4)$$

where $\boldsymbol{r}_\perp$ is the position of the lens relative to the undeflected line of sight to the source, $\boldsymbol{y}$ is the position of its image in the same plane, and α is the deflection angle times the angular size distance. In equation (3), a negative background convergence κ_b is included to account for the lack of background mass

[1] Present address: Department of Astrophysics, University of Oxford, Keble Road, Oxford OX1 3RH, England, UK.

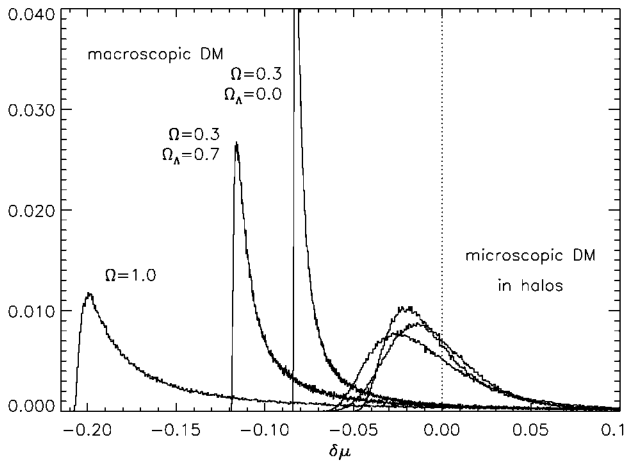

FIG. 1.—Histograms representing the total magnification probability distribution for macroscopic DM and microscopic DM clumped into halos. The means of all the distributions are zero. For the macroscopic DM case, all the matter in the universe is in the lenses. The shape of the distribution for DM halos is dependent on both the cosmology and the specific halo model assumed. This is a representative sample.

density that is assumed when D is used instead of $\tilde{D}$. Two magnifications, $\tilde{\mu}$ and μ, can be defined using equations (3) and (4), respectively. The requirement that the two lensing equations agree on the true size of an object results in the relation $\tilde{D}(\chi) = [1 - \kappa_b(\chi)]D(\chi)$. The explicit form of $\kappa_b(z)$ can be found by comparing the standard FLRW expression for $D(\chi)$ with the solutions for $\tilde{D}(\chi)$ found in Kantowski (1998).

The probability that the lens is located between $r_\perp$ and $r_\perp + dr_\perp$ is $p(r_\perp)dr_\perp \propto r_\perp dr_\perp$. If the lens is spherically symmetric and the magnification is a monotonic function of $r_\perp$, the expression for the magnification can be inverted (at least numerically) to get $r_\perp(\mu, D, D_s)$. Then, the probability of a lens causing the magnification $1 + \delta\mu$ can be found by changing variables. Lenses might also have properties such as mass, scale length, etc., which need to be averaged.

For the case of a point-mass lens, the total magnification of both images is given by $\tilde{\mu} = (\hat{r}^2 + 2)/[\hat{r}(\hat{r}^2 + 4)^{1/2}]$; $\hat{r} \equiv r_\perp/R_{\rm E}(m, D, D_s)$. The Einstein radius of the lens is given by $R_{\rm E}^2 = 4Gm\tilde{D}_l\tilde{D}_{ls}/\tilde{D}_s$. The single-lens distribution function is then

$$p(\delta\tilde{\mu})d\delta\tilde{\mu} \propto [(1 + \delta\tilde{\mu})^2 - 1]^{-3/2}\, d\delta\tilde{\mu}. \tag{5}$$

The probability in equation (5) is not normalizable; it diverges at small $\delta\tilde{\mu}$. This can be handled by introducing a cutoff in either $\delta\tilde{\mu}$ space or in $r_\perp$. The nature of this cutoff is not important as long as it is at sufficiently small $\delta\tilde{\mu}$ or large $r_\perp$. This will be clear when the total magnification distribution due to multiple lenses is considered.

If the DM consists of microscopic particles clumped into halos, the entire halo will act as a single lens. In this case, the Ricci focusing contribution to the magnification strongly dominates over shear distortions produced by mass outside of the beam (Holz & Wald 1998; Premadi, Martel, & Matzner 1998) and is then a function of only the local dimensionless surface density $\kappa(\boldsymbol{y})$. Furthermore, the lensing of the great majority of SNe will be quite weak, which allows us to confidently make the linear approximation: $\delta\mu = 2[\kappa(\boldsymbol{y}, D_l, D_s) + \kappa_b]$. This assumption has been well justified by many authors and will be confirmed by results in § 2.2.

For the purposes of this Letter, it will suffice to use a simple model for the surface density of halos. We use models with surface densities given by

$$\Sigma(y_\perp) = \frac{V_c^2}{2Gy_\perp}\left[\left(\frac{y_\perp}{r_s}\right)^2 + 1\right]^{-1}. \tag{6}$$

This model behaves like a singular isothermal sphere out to $y_\perp \simeq r_s$, where it is smoothly cut off.

In the following calculations, each halo is assumed to harbor a galaxy. At all redshifts, a Schechter luminosity function fit to local galaxies is assumed with $\alpha = -1.07$ and $\phi^* = 0.01(1 + z)^3 h^3$ Mpc^{-3}. The luminosities are then related to the circular velocity V_c by the local Tully-Fisher relation, $V_c = V_*(L/L_*)^{0.22}$, where $V_* = 200$ km s^{-1}. The scale lengths are related to the luminosity through $r_c = r_*(L/L_*)^{1/2}$ with $r_* = 220$ kpc. The precise values used for these parameters do not have a significant effect on the results of this Letter.

2.2. *Total Magnification*

The total magnification of a source includes contributions from all the lenses surrounding the light path. To find the true path connecting a source to us, the lensing equation must be solved with multiple deflections (see Schneider, Ehlers, & Falco 1992). The magnifications due to different lens planes are in general nonlinearly coupled. However, if the deflections due to no more than one of the lenses are very weak, the coupling between lenses can be ignored and their magnifications, $\delta\mu$ or $\delta\tilde{\mu}$, will add linearly. This is a good approximation for the vast majority of light paths in realistic models. The validity of this assumption will be justified by the results and is further investigated in Metcalf (1999). Furthermore, numerical simulations and analytic arguments show that for both kinds of DM it is a good approximation to take the lenses to be uncorrelated in space (see Holz & Wald 1998; Metcalf 1998b). If in addition we take the lenses' internal properties to be uncorrelated, the probability that the total magnification $\delta\tilde{\mu}_s$ of a point source is between $\delta\tilde{\mu}_s$ and $\delta\tilde{\mu}_s + d\delta\tilde{\mu}_s$ is

$$P(\delta\tilde{\mu}_s)d\delta\tilde{\mu}_s = d\delta\tilde{\mu}_s \int \prod_{i=1}^{N} [d\delta\tilde{\mu}_i\, p(\delta\tilde{\mu}_i)]\, \delta(\delta\tilde{\mu}_s - \sum_{i=1}^{N} \delta\tilde{\mu}_i), \tag{7}$$

where $\delta\tilde{\mu}_i$ is the contribution of the ith lens.

The magnification $\delta\mu_s$ is defined as the deviation of the luminosity from its mean value. As a result, the mean of the distribution $P(\delta\mu_s)$ must vanish.[2] This combined with the requirement that both magnifications agree on the true size of a source results in the expression $1 - \kappa_b(\chi) = \langle\tilde{\mu}(\chi)\rangle^{1/2}$. In this way the value of $\kappa_b(\chi)$ can be found by calculating the mean of equation (7) numerically, and a consistency check of the calculations can be made by comparing the results with the explicit values for $D(\chi)$ and $\tilde{D}(\chi)$. These values agree to a few percent, which is consistent with the uncertainty introduced by the discrete nature of the numerical calculation in the power-law tail of the distribution. The minimum magnification $\delta\mu_{\rm min}$ in the single-lens distribution is set low enough that the resulting total distribution is independent of the cutoff.

Figure 1 shows some examples of histograms made by pro-

[2] The actual mean angular size distance should be slightly larger than the FLRW value because galaxies obscure some sources. Galaxies are presumably correlated with high-density regions through which the magnification would be above average were they transparent.

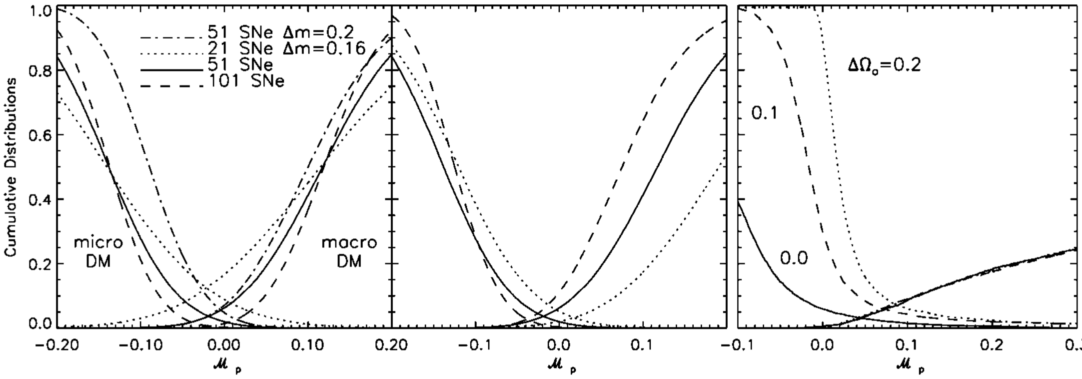

FIG. 2.—Differentiating DM candidates: the cumulative distributions of the statistic $\mathcal{M}_p$. The cases in which the true DM is macroscopic rise toward the right, and microscopic DM cases rise toward the left. All the observed SNe are taken to be at $z = 1$, and in all cases $\Omega_0 + \Omega_\Lambda = 1$ and $\Omega_\Lambda = 1$. *Left:* The different curves are for different numbers of observed SNe as marked with $\Delta m = 0.16$ mag in all cases except the dot-dashed curves. The halos have total density $\Omega_h = 0.27$. *Center:* The solid curves are the same as in the left panel, and the other curves are described in the text. *Right:* Here the cosmology is marginalized over Ω_0, with the widths of the prior Ω-distributions marked. In this case, there are 75 observed SNe.

ducing random values $\delta\tilde{\mu}_i$ drawn from the single-lens distributions and then adding them to get the total magnification. The macroscopic DM distributions shown in Figure 1 are independent of the lens mass and peak well below their mean and near the empty-beam solutions (corresponding to $\delta\mu = -0.21$, -0.12, and -0.084) because in these cases most lines of sight do not come very close to any lens. The probability that there are two lenses that individually give magnifications greater than $\delta\mu$ becomes appreciable only below the peak. This supports our approximation that whenever the lensing is strong it is dominated by one lens and the coupling between lenses is small at this redshift. In addition, we have compared our results with the numerical simulations of Holz & Wald (1998) and found excellent agreement.

3. DISTINGUISHING DARK MATTER CANDIDATES

The apparent luminosity of an SN, $l_{\rm ob}$, after lensing can be expressed in terms of either of the two magnifications, $l_{\rm ob} = \mu l = \tilde{\mu} l / \langle\tilde{\mu}\rangle$. We wish to infer via the measured luminosities of a set of SNe, each located at a different redshift, from which distribution the magnifications were drawn and in this way surmise which DM candidate is most likely. To establish some insight into the magnitude of this effect, the differences in magnitudes between the average and the empty-beam solutions at $z = 1$ are -0.25 mag for $\Omega_0 = 1$, -0.14 mag for flat $\Omega_0 = 0.3$, and -0.10 mag for open $\Omega_0 = 0.3$.

Let us denote the probability of getting a data set $\{\delta\mu\}$ given a model—either microscopic or macroscopic DM—as $P(\{\delta\mu\}|\text{model}) = \prod_i P(\delta\mu_i|\text{model}) d\delta\mu_i$, where the product is over the observed SNe. The model here includes sources of noise. This probability can be calculated numerically from the probability distributions discussed in § 2.2. Because of Bayes's theorem, we know that the ratio of these two probabilities is equal to the relative likelihood of the models being correct, i.e., the odds, given a data set. It is convenient to modify the odds into the statistic

$$\mathcal{M}_p \equiv \frac{1}{N_{\rm SN}} \ln\left[\frac{\int d\Omega_0 d\Omega_\Lambda\, p(\Omega_0,\Omega_\Lambda) P\left(\{\delta\mu\}|\text{macroDM, noise}\right)}{\int d\Omega_0 d\Omega_\Lambda\, p(\Omega_0,\Omega_\Lambda) P\left(\{\delta\mu\}|\text{halos, noise}\right)}\right], \tag{8}$$

where $p(\Omega_0, \Omega_\Lambda)$ is the prior distribution for the cosmological model based on independent information or prejudice. The measured $\mathcal{M}_p$ is expected to be large if DM is macroscopic and smaller if DM is microscopic or nonexistent.

For the left panel in Figure 2, 5000 simulated data sets were created, $\mathcal{M}_p$ was calculated for each of them, and their cumulative distributions were plotted. The noise included in the simulation originates from both the intrinsic distribution of SN luminosities, presently corrected to ~0.12 mag, and the observational noise, presently an additional ~0.08 mag. For the left panel, the noise is taken to be Gaussian distributed in magnitudes with a standard deviation of 0.16 mag, except for the dot-dashed curves which have $\Delta m = 0.2$ mag. The cosmology is fixed in this plot, i.e., $p(\Omega_0, \Omega_\Lambda)$ is a δ-function. $\mathcal{M}_p$ can be calculated for a given data set and compared to this plot to determine its significance. It can be seen here that for 51 SNe (*solid curve*) at $z = 1$, the two distributions overlap at the 4% level, i.e., 96% of the time one of the DM candidates can be ruled out at better than the 96% confidence level. One of the advantages of $\mathcal{M}_p$ is that it is close to Gaussian distributed with a mean that is independent of the number of SNe observed. In this way, once the cosmology and noise model is fixed, the value of $\mathcal{M}_p$ is a direct prediction of the kind of DM.

The middle panel in Figure 2 illustrates the importance of some possible systematic uncertainties that arise from not knowing precisely the distribution of the noise. The solid curves are the same as in the left panel. The dotted curve is the extreme case in which the noise is actually Gaussian distributed in magnification (there is a low-magnitude tail), but $\mathcal{M}_p$ is calculated under the same assumptions as in the left panel. The dashed line in this panel is the case in which the standard deviation is overestimated to be $\Delta m = 0.2$ mag but is really $\Delta m = 0.16$ mag. These errors in the noise model do not destroy the efficacy of the test, but they could be important if a long tail exists in the intrinsic distribution of luminosities, and they become more important for smaller Ω_0 and Ω_Λ.

The right panel in Figure 2 addresses the question of differentiating between DM candidates without assuming specific values for the cosmological parameters, thereby making the conclusion cosmology independent. Here the prior is taken to be $p(\Omega_0, \Omega_\Lambda) = \delta(1 - \Omega_0 - \Omega_\Lambda)$ within a range in Ω_0 ($\Delta\Omega_0 = 0$, 0.1, and 0.2) centered on 0.3 and zero otherwise. The simulated data is the same here as for the solid curves in the other two panels. However, the integrations in equation (8) would be prohibitively time consuming if the entire magnification distribution function were calculated for each trial cosmology. To simplify the calculation without losing much of the test's effectiveness, we use approximate, analytic test distribution functions. For the macroscopic DM case, we use equation (5) with the low-magnification cutoff, which ensures that it gives the correct mean. Comparison of this approximation with the full multilens distribution shows that it is a good approximation, especially for low Ω_0. For the microscopic DM/halo case, we approximate the distribution as a Gaussian with an appropriate width (see Metcalf 1998a). This plot shows that not only is this simplified calculational technique adequate, but that one does not need to assume a precise cosmological model to differentiate between DM candidates. Increasing the width of the prior beyond $\Delta\Omega_0 = 0.2$ does not make much difference. The reason for this is that if the assumed cosmological parameters are significantly different than the true ones, the distribution will be shifted to an extent that it is no longer consistent with the data. This shift would be confused for a lensing effect if the two kinds of distributions, illustrated in Figure 1, were translations of each other, but they are not, even after noise is added. For the two DM cases, the modes of the magnification distributions follow different *m*-*z* relations, but their means are the same. For a fixed redshift, it is the distribution of luminosities about the mean that distinguishes the two cases.

For open models ($\Omega_\Lambda = 0$), it is more difficult to differentiate the DM candidates, but even in this case with 51 SNe at $z = 1$ and $\Omega_0 = 0.3$ we expect to get better than 90% confidence at least 90% of the time. If $\Omega_0 = 0.1$, BBN constraints just barely allow for all DM to be made of baryonic objects. In this case, similar bounds to those shown in Figure 2 for 51 SNe can be achieved with 200 SNe. However, the means of the $\mathcal{M}_p$ distributions are closer together in this case, making the test more susceptible to systematic errors in the assumed noise model.

The power of lensing to differentiate DM candidates comes mostly from its ability to identify macroscopic DM. A positive detection of the lensing by microscopic DM halos will take more SNe, as will constraining the precise fraction of DM in macroscopic form, unless correlations between SN luminosities and foreground galaxies are utilized (Metcalf 1998b, 1999).

4. DISCUSSION

One concern in implementing the test described here is the possibility that Type Ia SNe and/or their galactic environments evolve with redshift. This is also a major concern in cosmological parameter estimation from SNe. So far there is no indication that the colors or spectra systematically change with redshift (Perlmutter et al. 1997; Riess et al. 1998). Since the evolution of the magnification distribution is determined by cosmology, it is in principle possible to make an independent test for systematic evolution in the distribution of SN luminosities.

Microscopic DM does not need to be clustered for this test to work. The clustering is added to make the calculations realistic. Clustering the microscopic DM to a greater or lesser extent would affect our results quantitatively, but the test would still be viable in more extreme cases. We conclude that if the assumptions we have made about the noise levels in future SN observations remain reasonable, on the order of 50–100 SNe at $z \sim 1$ should suffice to determine a fundamental question: whether the major constituent of extragalactic DM is microscopic particles or macroscopic objects.

We would like to thank D. Holz for providing the results of his simulations for the purposes of comparison.

REFERENCES

Dyer, C. C., & Roeder, R. C. 1974, ApJ, 189, 167
Holz, D. E., & Wald, R. M. 1998, Phys. Rev. D, 58, 063501
Kantowski, R. 1998, ApJ, 507, 483
Metcalf, R. B. 1998a, MNRAS, 305, 746
———. 1998b, in Evolution of Large-Scale Structure: From Recombination to Garching, ed. A. J. Banday, R. K. Sheth, & L. N. da Costa (Enschede: Print Partners Ipskamp), in press
———. 1999, in preparation
Patat, F., Benetti, S., Cappellaro, E., Danziger, I. J., Della Valle, M., Mazzali, P. A., & Turatto, M. 1996, MNRAS, 278, 111
Perlmutter, S., et al. 1997, ApJ, 483, 565
Premadi, P., Martel, H., & Matzner, R. 1998, ApJ, 493, 10
Riess, A. G., et al. 1998, AJ, 116, 1009
Schneider, P., Ehlers, J., & Falco, E. E. 1992, Gravitational Lenses (Berlin: Springer)
Schneider, P., & Wagoner, R. V. 1987, ApJ, 314, 154